Use of the Relaxation Function in the Nuclear Magnetic Resonance Analysis of Internal Motions in Solids

EDWIN M. ROBERTS
Lockheed-Georgia Company, Marietta, Georgia 30060
AND
CHARLES W. MERIDETH
Lockheed-Georgia Company, Marietta, Georgia 30060
and
Morehouse College, Atlanta, Georgia 30314
(Received 8 July 1968)

The motional narrowing of nuclear-magnetic-resonance spectra is examined from the point of view of Anderson. The relaxation function, which is the Fourier transform of the absorption spectrum, is used to connect the experimental data with the stochastic model of the motion. The interaction of the spins with their surroundings is treated as a stochastic process of the nature of a random telegraph signal with random amplitudes. The possibility of incomplete narrowing is easily included. Two theoretical relaxation functions are developed. The first function is derived from the assumption of a normal distribution for the phase deviation, and the second results from a uniformly distributed phase deviation. Ammonium chloride and titanium hydride are studied experimentally. The two theoretical relaxation functions are compared with the experimental relaxation function. The relaxation function based on a uniformly distributed phase deviation is in best agreement with experiment. Arrhenius activation energies are calculated and compared to those obtained from linewidth data. The apparent second moment is related to the frequency of motion. The relation has the advantage of internal consistency and is not contingent on an assumed line shape. The activation energies obtained from second-moment data are practically the same as those obtained by the relaxation-function method. The correction for the effect of modulation on the relaxation function is derived. This correction leads naturally to a relation between the observed line shape and the actual line shape. Partial experimental verification of the theory of modulation broadening is given.

I. INTRODUCTION

MOTIONS such as molecular rotation, diffusion, and chemical exchange affect the several quantities which describe nuclear magnetism.[1] In most instances, the resonance curve is sharply and monotonically narrowed by the motion of the spins to a width considerably less than the width in the absence of motion. Generally, the shape of the NMR spectrum is sensitive only to those motions with characteristic frequencies greater than or equal to the rigid lattice linewidth. The relaxation time T_1 is sensitive to both low- and high-frequency motions. Consequently, relaxation-time measurements are informative over a larger temperature range than are the linewidth measurements. Nevertheless, continuous-wave data over the temperature range in which the line shape narrows contains important information regarding the motion responsible for the narrowing.

The connection between line narrowing and random motion which may occur in condensed phases was first given by Bloembergen, Purcell, and Pound.[1] Although the BPP theory describes the experimental data rather well, it fails to make full use of the experimental line shape. The theoretical explanation of motional narrowing has been improved by Kubo and Tomita,[2] but the underlying physical picture of the effect as given by BPP is undoubtedly correct. A recent rigorous theory of spin resonance and relaxation which describes motional narrowing has been given by Argyres and Kelley.[3]

An experimental approach to motional narrowing could be based on Anderson's elegant theory.[4] In this theory, the Fourier transform of the resonance spectrum is the quantity which reflects the motion of the spins. We will call the Fourier transform of the resonance spectrum the "relaxation function," or more briefly, $G(t)$. The advantages of working in the time domain with $G(t)$ are both theoretical and experimental. First, the dynamical or temporal behavior of the local field experienced by the spins is of primary interest rather than the average of the absolute value of the local field, although the latter, more naturally evident in the line shape, is also of interest. Second, as Anderson clearly states, the moments of the shape function are determined by the behavior of $G(t)$ very near the time origin, and they have very little to do with its general course. For example, the second moment of the shape function is actually independent of any temporal behavior of the local field, whereas the fourth moment would be theoretically expected to increase as the fluctuations in the local field become more rapid. Experimentally, the second and fourth moments appear to decrease as a result of motion. This apparent discrepancy arises because, for a narrowed resonance, the wings of the spectrum contribute large portions to the moments. On the other hand, the Fourier transform

[1] N. Bloembergen, E. M. Purcell, and R. V. Pound, Phys. Rev. 73, 679 (1948). Hereafter referred to as BPP.
[2] R. Kubo and K. Tomita, J. Phys. Soc. Japan 9, 888 (1954).
[3] P. N. Argyres and P. L. Kelley, Phys. Rev. 134, A98 (1964).
[4] P. W. Anderson, J. Phys. Soc. Japan 9, 316 (1954).

of the spectral shape, being the average value of a function with unit modulus, will have relatively smaller contributions from the wings. The calculation of $G(t)$ from the observed spectral line shape will be more accurate than the calculation of spectral moments while still making optimum use of the line shape.

It should also be pointed out that, since $G(t)$ is also the shape of the free-induction decay,[5] an independent check on cw data is available.[6] Under certain circumstances, it may be that free induction will be the superior method for obtaining $G(t)$. A practical example is that the calculation of $G(t)$ from cw data involves considerable labor, whereas, ideally, free-induction decay produces $G(t)$ directly.

In this paper Anderson's basic theory is applied to two systems which exhibit motional narrowing. These systems, which have been previously studied by other investigators, were chosen as being representative of the various types of motions which can be studied conveniently by magnetic-resonance methods.

II. THEORY

A. Anderson's Theory

A brief resume of Anderson's theory of motional narrowing as recast by Abragam[7] will be useful. A collection of nuclear spins is described by a Hamiltonian H, which consists of a Zeeman term, a smaller term H_1, which is responsible for the line broadening, and a term F, pertaining to the motion of the atoms or molecules which carry the spins. Let μ_x denote the x component of magnetization, and define $\mu_x(t)$ by[8]

$$\mu_x(t)=e^{iHt}\mu_x e^{-iHt}. \tag{1}$$

It may be shown that the shape function $g(\omega)$ is given by

$$g(\omega)=\frac{1}{\pi}\int_0^\infty \mathrm{Tr}[\mu_x(t)\mu_x]\cos\omega t dt. \tag{2}$$

The frequency ω is the deviation from the resonant frequency. The quantity $\mathrm{Tr}[\mu_x(t)\mu_x]$, the relaxation function, will be denoted by $G(t)$. By inverting (2), we have

$$G(t)=2\int_0^\infty g(\omega)\cos\omega t d\omega. \tag{3}$$

Since F and H_1 do not commute, a time dependence is impressed on H_1, which may be expressed by the relation

$$H_1(t)=e^{-iFt}H_1 e^{iFt}. \tag{4}$$

Because the concern here is only with observations on the spin system, the lattice is evident only through its effect on the spin system. It is then appropriate to treat $H_1(t)$ as a random operator.

The final expression for $G(t)$ is

$$G(t)=E\left[\exp i\int_0^t \omega(t)dt\right], \tag{5}$$

where

$$\omega(t)=\langle m|H_1(t)|m\rangle-\langle n|H_1(t)|n\rangle. \tag{6}$$

In (6), the states $|m\rangle$ and $|n\rangle$ have Zeeman frequencies which differ by the resonance frequency. Further, in (5), the notation $E[X]$ is used to denote the expectation of the random variable X over an appropriate probability distribution.

The integral which occurs in (5) has a simple physical interpretation. It is the resultant phase deviation of the spin system as would be observed from the rotating frame over a time interval t. The phase deviation is denoted by $\Phi(t)$.

The probability distribution of $\omega(t)$ is not given by the above theory. A distribution must be chosen from *a priori* considerations and then tested against experiment.

B. Stochastic Model

In those cases of interest, H_1 may be written as a sum:

$$H_1=\sum_{i=1}^{N}\sum_{\alpha} U_i^{(\alpha)}(x)V_i^{(\alpha)}(s), \tag{7}$$

where $U_i^{(\alpha)}(x)$ refers to an individual spin i, and is a function of the kind α of the spatial coordinates of the spins, and $V_i^{(\alpha)}(s)$ is a spin operator. It is now assumed that the transformation (4) has the effect of simply introducing a random time dependence into the lattice variables x.[7] The lattice is now to be treated as a classical system.

In arriving at a description of the stochastic process $\omega(t)$, the ideas developed by Pines and Slichter[9] are followed very closely. Suppose we could count the number of changes in $\omega(t)$ during the time interval $(0,t)$. This number will be denoted by $n(t)$. We define $n(0)=0$. We would expect that the counts corresponding to two nonoverlapping time intervals will be statistically independent. That is, if $t_3>t_2>t_1$, the random variables $n(t_2)-n(t_1)$ and $n(t_3)-n(t_2)$ are independent. The justification of this assumption is found in the fact that changes in $\omega(t)$ have negligible reciprocal action on the lattice variables. Secondly, we assume that for $t_2>t_1$ and any $\tau>0$, the random variables $n(t_2)-n(t_1)$ and $n(t_2+\tau)-n(t_1+\tau)$ are identically distributed. The last assumption is a natural way of statistically describing the absence of trends in $\omega(t)$. The next assumption must be considered as an idealization. It is assumed that only a finite number of

[5] I. J. Lowe and R. E. Norberg, Phys. Rev. **107**, 46 (1957).
[6] H. A. Resing, J. Chem. Phys. **37**, 2575 (1962).
[7] A. Abragam, *The Principles of Nuclear Magnetism* (Oxford University Press, London, 1961), Chap. X.
[8] By convention $\hbar=1$.
[9] D. Pines and C. P. Slichter, Phys. Rev. **100**, 1014 (1955).

counts occur in any finite time interval. Finally, since $\omega(t)$ refers to the entire spin system, it is obvious that no more than one count is registered at any instant of time. The four conditions placed on $n(t)$ in the above discussion uniquely define the stochastic process $n(t)$ as a Poisson process.[10] Thus, for $n(t)$, we postulate the probability distribution

$$P(n(t)=k)=((\nu t)^k/k!)e^{-\nu t}, \tag{8}$$

where the parameter ν determines the average number of counts in time t according to

$$E(n(t))=\nu t. \tag{9}$$

The mean rate ν with which changes in $\omega(t)$ occur is related to the rate with which changes in the lattice variables are occurring. However, the two rates are not necessarily the same. To see this, suppose the number of times the spins change lattice positions is given by a Poisson distribution with mean rate λ. It is possible that two distinct spatial configurations of the spins have the same value of $\omega(t)$. Suppose each change in spatial configuration has a probability $p\leq 1$ of causing a change in $\omega(t)$. Then changes in $\omega(t)$ will occur in accordance with a Poisson distribution with mean rate $\nu=p\lambda$. An experimental determination of ν will give only a lower bound to the jump frequency λ.

At any instant, the probability distribution of $\omega(t)$ is symmetric about zero. The changes in $\omega(t)$ will be both positive and negative as time proceeds, and the ensemble averages of $\omega(t)$ and $\omega(t)^2$ will be zero and finite, respectively. A reasonable model of $\omega(t)$ is a step function with both positive and negative steps of random magnitudes. A stochastic process with this behavior is

$$\omega(t)=A\exp[i\pi n(t)]+B, \tag{10}$$

where $n(t)$ is the Poisson process and A and B are random variables independent of time. The random variable A represents a part of $H_1(t)$ that is affected by the motion; B is not affected. It is assumed that A and B have zero means and finite second moments. A further simplification results if it is assumed that $n(t)$, A, and B are mutually independent. The process (10) is similar to the random telegraph signal.[11]

The covariance of $\exp[i\pi n(t)]$ for events occurring in the interval $0\leq t_1\leq t_2$ is

$$\begin{aligned} K_n(t_2,t_1)&=E\{\exp[i\pi n(t_2)]\exp[i\pi n(t_1)]\}\\ &=E\{\exp[i\pi n(t_2-t_1)]\}, \end{aligned} \tag{11}$$

where, in the final expression, the decomposition of $n(t_2)$ into $n(t_1)+n(t_2-t_1)$ has been used. Using Eq. (8) we have

$$\begin{aligned} K_n(t_2,t_1)&=\sum_k [P(n(t_2-t_1)=\text{even } k)\\ &\qquad -P(n(t_2-t_1)=\text{odd } k)]\\ &=\left[\sum_{k\text{even}}\frac{\nu^k(t_2-t_1)^k}{k!}-\sum_{k\text{odd}}\frac{\nu^k(t_2-t_1)^k}{k!}\right] \qquad (12)\\ &=e^{-2\nu(t_2-t_1)},\quad t_2\geq t_1. \end{aligned}$$

We remove the restriction $t_2\geq t_1$, and write

$$K_n(t_2,t_1)=e^{-2\nu|t_2-t_1|}. \tag{13}$$

The covariance of $\omega(t)$, $E(\omega(t_2)\omega(t_1))$, is denoted by $K_\omega(t_2,t_1)$. We have

$$K_\omega(t_2,t_1)=\sigma_A{}^2K_n(t_2,t_1)+\sigma_B{}^2, \tag{14}$$

where $\sigma_A{}^2$ and $\sigma_B{}^2$ are the second moments of A and B.

The phase deviation, discussed in connection with Eq. (5), is

$$\Phi(t)=\int_0^t\omega(s)ds. \tag{15}$$

The first and second moments of $\Phi(t)$ may be computed easily. For the first moment,

$$E(\Phi(t))=\int_0^t E(\omega(s))ds=0. \tag{16}$$

For the second moment,

$$\begin{aligned} E(\Phi^2(t))\equiv\varphi^2&=E\left\{\int_0^t\omega(t_2)dt_2\int_0^t\omega(t_1)dt_1\right\}\\ &=\int_0^t\int_0^t E[\omega(t_2)\omega(t_1)]dt_2dt_1\\ &=\sigma_A{}^2\int_0^t\int_0^t K_n(t_2,t_1)dt_2dt_1+\sigma_B{}^2t^2. \end{aligned}$$

If $t>0$, the second moment is

$$\varphi^2=(2\sigma_A{}^2/\alpha^2)[e^{-\alpha t}-1+\alpha t]+\sigma_B{}^2t^2, \tag{17}$$

where $\alpha=2\nu$.

Continuing with the ideas of Pines and Slichter,[9] defining T_2 as the time for which $\varphi^2=1$, then

$$1=\sigma_B{}^2T_2{}^2+(2\sigma_A{}^2/\alpha^2)[e^{-\alpha T_2}-1+\alpha T_2]. \tag{18}$$

In loose terms, $(2/T_2)$ is the linewidth, and Eq. (18) could be treated as an alternate to the BPP equation[1]:

$$\left(\frac{1}{T_2'}\right)^2=\left(\frac{1}{T_2''}\right)^2\frac{2}{\pi}\tan^{-1}\frac{2\tau_c}{T_2'}. \tag{19}$$

Equation (19) is written in the notation of Ref. 1.

[10] J. L. Doob, *Stochastic Processes* (John Wiley & Sons, Inc., New York, 1953), Chap. VIII, p. 398.

[11] S. O. Rice, Bell System Tech. J. 23, 282 (1944).

In the rigid lattice case, $1/T_2^2$ is equal to $\sigma_A^2+\sigma_B^2$, which is the rigid lattice second moment. In the case of very rapid motion, $1/T_2^2$ approaches σ_B^2, which is the apparent second moment of the narrowed line.

To compute $G(t)$, the probability distribution of $\Phi(t)$ must be known. If $\Phi(t)$ were normally distributed, we could immediately write

$$G(t)=\exp(-\tfrac{1}{2}\varphi^2). \tag{20}$$

It might be hoped that, by assuming A to be normally distributed, $\omega(t)$ would be a normal process. Although it can be shown that this is not true, Eq. (20) will be a good approximation for times such that $\varphi^2\leq 1$. In what follows, the function (20) will be denoted by $G_1(t)$.

Another justification for Eq. (20) is found in a general theorem on second-order stochastic processes,[12] which ensures us of the existence of a normal process having the same covariance as $\omega(t)$. Thus, in a model involving only means and covariances, there is no loss in assuming $\omega(t)$ to be a normal process. This theorem actually provides a rigorous basis for the discussion given in the last paragraph.

Another useful relaxation function is obtained by assuming that $\Phi(t)$ at any time is uniformly distributed with mean square given by (17). It may be that such an assumption is not consistent with the stochastic model for $\omega(t)$. If this rather difficult mathematical question is ignored, the assumption of a uniformly distributed phase deviation leads to a second functional form for $G(t)$,

$$G_2(t)=\sin(3\varphi^2)^{1/2}/(3\varphi^2)^{1/2}. \tag{21}$$

The stochastic model developed above is perhaps the simplest which realistically describes motional narrowing. The model suffers from having only one adjustable parameter. Equation (10) may be modified to include several narrowing processes corresponding to the excitation of different degrees of freedom. An example of multiple narrowing processes is found with 1,1,1-trichloroethane.[13] A further generalization would be the inclusion of several kinds of interactions which are destroyed by motion. For example, H_1 might include dipole-dipole and nuclear quadrupole interactions. While these modifications might be necessary in special cases, the model remains essentially a one-parameter model.

Several recent contributions to the problems of line-shape analysis and motional narrowing have appeared. Fixman[14] and Saunders and Johnson[15] apply Monte Carlo techniques to the numerical calculation of the relaxation function for systems governed by the classical rotational diffusion model containing one diffusion coefficient. Sillescu and Kivelson[16] develop an elaborate theory of magnetic-resonance line shapes which includes both secular and nonsecular spin-lattice interactions. The latter work is also restricted to a single diffusion coefficient.

Additional parameters for a single process can be introduced in several ways. One way is suggested by the formula relating the rigid lattice fourth moment to the fourth moment of the narrowed line,[4,7]

$$M_4=M_4^0+K_\omega''(t,t). \tag{22}$$

$K_\omega''(t,t)$ is the second derivative of $K_\omega(t,t')$ evaluated at $t=t'$. If $K_\omega''(t,t)$ exists, it is positive and is the covariance of a stochastic process $\omega'(t)$ which has the significance of the rate of change of $\omega(t)$. In the case of the model discussed above, $K_\omega''(t,t)$ does not exist, so $\omega'(t)$ does not exist. This suggests that a stochastic process be constructed to describe $\omega'(t)$.

III. EXPERIMENTAL APPARATUS AND PROCEDURE

A. Apparatus

The apparatus used was a Varian VF-16 wide-line spectrometer operable over a frequency range of 2 to 16 MHz. The magnet system was a V-3603 12-in. electromagnet regulated by a Field Dial. The recording system consisted of a C1024 time-averaging computer (TAC) and a Houston model 6550 omnigraphic recorder. All frequencies and periods were measured with a Hewlett-Packard model 5245-L electronic counter. The sample temperature was regulated with a V-4557 variable-temperature accessory adapted for use in the wide-line probes.

B. Spectra

The spectra were recorded using scanning speeds ranging from 0.004 to 0.035 G/sec. The phase-detected signal for each scan was stored in the TAC. The TAC was triggered externally at the beginning of each scan. The channels of the TAC were advanced by a square wave externally derived from a Hewlett-Packard 3300-A function generator. The channel advance rate was chosen such that the sweep time of the TAC was very slightly less than the sweep time of the Field Dial. Small but measurable long-term drifts in magnetic field were cancelled, when necessary, by moving the position of a narrow resonance line to the center of the sweep range.

At the completion of the desired number of scans the time-averaged spectrum was read out on the Houston recorder. The recorder controlled the data-source scan rate. The curves were symmetrized by the method of Bruce.[17] The spectral data were then converted to

[12] J. L. Doob, *Stochastic Processes* (John Wiley & Sons, Inc., New York, 1953), Chap. II, p. 74.

[13] H. S. Gutowsky and G. E. Pake, J. Chem. Phys. **18**, 162 (1950).

[14] Marshall Fixman, J. Chem. Phys. **48**, 223 (1968).

[15] Martin Sauders and Charles L. Johnson, Jr., J. Chem. Phys. **48**, 534 (1968).

[16] Hans Sillescu and Daniel Kivelson, J. Chem. Phys. **48**, 3493 (1968).

[17] C. R. Bruce, Phys. Rev. **107**, 43 (1957).

digital form with a graphic-data digitizer for the purpose of computer processing.

C. Calibrations

In order to correct experimental results for the effects of field modulation, the amplitude of the modulation field must be known. The peak-to-peak amplitude of the modulation field was measured by adjusting the resonant frequency of doped water to coincide with the extremes of the modulated field.

The scanning rates, i.e., $\gamma \dot{H}_0$, were calibrated by scanning through a narrow resonance line at two different radio frequencies. The two scans were stored successively in the TAC and then jointly displayed on the recorder. The scanning rate is proportional to the scale on the chart paper divided by the channel advance period.

All samples were sealed in glass tubes along with a small amount of argon. The Pyrex sample tubes were 8.5 mm in i.d. A capillary, which served as a thermocouple well, entered the top of the tube through a ring seal. The closed bottom of the capillary was 2 cm from the bottom of the sample tube. This arrangement allowed the temperature to be measured at a point within the sample near the center of the receiver coil.

The temperature of a sample was measured by means of a copper-constantan thermocouple having a Teflon insulation. The temperature was measured before and after each scan. If a discrepancy of over 1° occurred, the spectrum was discarded. The possibility of short-term fluctuations in temperature was investigated at several temperatures by monitoring the thermocouple emf with a recording potentiometer. The results showed a rather remarkable stability of 0.1° over periods as long as 2 h. It was observed that spurious signals appeared in the TAC if temperature measurements were attempted during a scan of the spectrum. Therefore, temperature was not monitored during a scan period.

D. Calculations

Second moments, fourth moments, and Fourier transforms of the spectral lines were obtained by numerical integration. The effect of magnetic field modulation was accounted for in the calculations. The relations between the uncorrected and corrected quantities are as follows:

$$M_2' = M_2 + b^2/4, \tag{23a}$$

$$M_4' = M_4 + 3b^2 M_2/2 + b^4/8, \tag{23b}$$

$$F(t) = [2J_1(bt)/bt]G(t), \tag{23c}$$

where M_2', M_4', and $F(t)$ are the uncorrected quantities. $J_1(bt)$ is the first-order Bessel coefficient and

$$b = \tfrac{1}{2}\gamma H_m, \tag{24}$$

where H_m is the peak-to-peak magnitude of the modulation field in gauss and γ is the gyromagnetic ratio. A derivation of (23c) is given in the Appendix.

The Fourier transform of the shape function was obtained from the first derivative of the observed line shape $f(\omega)$ by numerical evaluation of the integral

$$F(t) = 2\int_0^{\Omega} f'(\omega)\frac{\sin\omega t}{t}d\omega,$$

where Ω is a number such that $f'(\omega)$ is effectively zero for $\omega > \Omega$. In several instances, it was found that $F(t)$ was oscillatory in behavior and possessed zeros not all of which were identical with the zeros of $J_1(bt)$. There are two possible explanations for these additional zeros. First, $G(t)$ may have an oscillatory behavior. Second, the appearance of additional zeros due to truncation is always to be expected by analogy to the Gibbs phenomenon of a Fourier series of a discontinuous function. Computations which will not be reproduced have indicated that the additional zeros in $F(t)$ due to truncation at Ω occur at times much larger than the zeros observed for rigid lattice spectra. The additional zeros must then arise from $G(t)$. However, all additional zeros which are observed for motionally narrowed spectra might possibly be due to truncation.

IV. RESULTS AND DISCUSSION

A. Ammonium Chloride

NMR has shown conclusively that the ammonium ions of an ammonium halide undergo random reorientations.[18] These reorientations occur well below the λ point. The ammonium halides offer textbook examples of the utility of magnetic resonance in revealing thermal motions which occur too infrequently to be detected by ordinary thermodynamic methods.

The experimental second moments for the low- and high-temperature plateaus were found in this work to be $(4.02\pm0.04)\times10^{10}$ and $(0.22\pm0.01)\times10^{10}$ sec^{-2}, respectively. These values differ by about 10% from the values 3.54×10^{10} and 0.24×10^{10} sec^{-2} reported by Gutowsky *et al.* The fourth moment decreases from a rigid lattice value of 32.00×10^{20} sec^{-4} to a low of 0.12×10^{20} sec^{-4}. The rigid lattice line shape shows evidence of fine structure. If this fine structure is neglected, the rigid lattice line shape may be described as being somewhat flatter on top than a Gaussian curve, as indicated by the ratio $M_4/M_2^2 = 1.98$. The shape of the narrowed line shows no fine structure.

For a given temperature, the time T_2 was taken from the experimental relaxation function as the time for which

$$G(T_2) = e^{-1/2}.$$

[18] H. S. Gutowsky, G. E. Pake, and R. Bersohn, J. Chem. Phys. 22, 643 (1954).

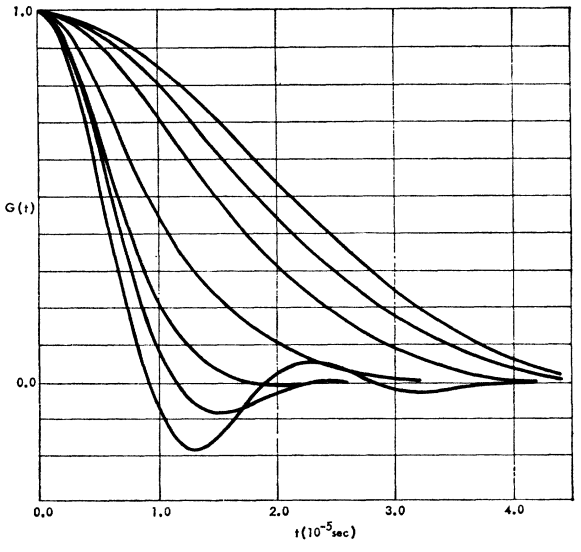

FIG. 1. Experimental relaxation functions $G(t)$ for NH_4Cl. The sequence of curves from left to right corresponds to the temperature sequence T°C= −163, −153, −148, −141, −135, −130, and −126.

The corresponding frequency α was then obtained by solving Eq. (18). The results are given in Table I.

Previous observations[18] have indicated differences in line shape in the transition region depending on whether the sample was warmed or cooled to arrive at the final temperature. The experimental data reported here indicates the same behavior at −141°C, which is near the midpoint of the transition region. At that temperature, T_2 is significantly larger when equilibrium is approached from below than when approached from above. This behavior was not noticeable at the other temperatures. Because of the rapidity with which the line shape changes near −141°C, it is difficult to determine if the discontinuity in T_2 is real or only apparent due to a lag in attaining temperature equilibrium throughout the sample.[18]

Figure 1 shows the experimental relaxation function for seven temperatures in the transition region. The qualitative behavior of T_2 increasing with temperature is as predicted from simple considerations of conjugate Fourier transforms.[4] The oscillations or beats exhibited by $G(t)$ at or near rigid lattice conditions are due in part to the fine structure[19] and, in part, to an effect first observed by Lowe and Norberg.[5] They observed beats in the free-induction decay of solids which exhibit no fine structure. At temperatures below −160°C, the beats exhibited by NH_4Cl have an angular frequency of 3.5×10^5 rad sec^{-1}.

Figure 2 shows a comparison of the experimental $G(t)$ with $G_1(t)$. The relative difference

$$\epsilon_1=[G_1(t)-G(t)]/G(t)$$

is also shown in Fig. 2.

A graph of $\log_{10}\alpha$ versus $10^3/T$ shown in Fig. 3 indicates that the temperature dependence of α is described by the Arrhenius equation

$$\alpha=\alpha_\infty \exp(-E/RT), \tag{25}$$

where E is an activation energy related to the reorientation of the ammonium ion.

Also shown in Fig. 3 is a plot of $\log_{10}(1/\tau_c)$ versus $10^3/T$, where τ_c is the correlation time calculated from linewidth data and the equation[20]

$$(1/T_2')^2=\delta_B^2+C\sigma_A^2\tan^{-1}(\tau_c/CT_2'). \tag{26}$$

In Eq. (26), C is 0.883 and $2/T_2'$ is the width of the absorption curve between inflection points. The minimum linewidth is denoted by $2\delta_B$. Again an Arrhenius activation energy was calculated. The results of the two theories are compared in Table II. Also shown are the values computed from T_1 data.[21]

TABLE I. Values of T_2, α, and M_2 for NH_4Cl throughout the transition region. T_2 is the time for which the experimental G is $e^{-1/2}$. α is then calculated from Eq. (18). All values are corrected for modulation effects.

T (°C)	T_2 (10^{-5} sec)	α (10^5 sec^{-1})	M_2 (10^{10} sec^{-2})
≤−163	0.50	···	4.02
−153	0.54	0.96	3.43
−148	0.59	1.96	3.04
−141[a]	0.97	8.07	1.08
−141[b]	0.79	5.44	1.76
−135	1.28	14.40	0.66
−130	1.58	26.00	0.42
−126	1.85	56.50	0.30
+ 26	2.07	···	0.22

[a] Temperature attained by warming.
[b] Temperature attained by cooling.

B. Titanium Hydride

The self-diffusion of hydrogen in titanium hydride of various compositions has been examined by Stalinsky *et al.*[22] Their results show: (1) The hydrogen atoms are located at random tetrahedral positions with respect to the titanium atoms, and (2) the diffusion takes place by way of a vacancy mechanism.

A sample of commercially obtained titanium hydride was used in this work. Chemical analysis gave a composition corresponding to $TiH_{1.94}$ with less than 0.23% impurity by weight. The rigid lattice second moment was found to be $(1.83\pm0.03)\times10^{10}$ sec^{-2}, which is in good agreement with the values reported in Ref. 22. The corresponding fourth moment was $(8.70\pm0.4)\times10^{20}$ sec^{-4}. The rigid lattice line shape is only approximately Gaussian, as indicated by the ratio M_4/M_2^2.

[19] T. P. Das and S. K. Ghosh Roy, Indian J. Phys. 29, 272 (1955).
[20] Equation (26) is the equation of Kubo and Tomita [Ref. 2, Eq. (6.27a)] extended to include the possibility of incomplete motional averaging.
[21] G. E. Pake, in *Solid State Physics*, edited by F. Seitz and D. Turnbull (Academic Press Inc., New York, 1956), Vol. 2.
[22] B. Stalinsky, C. K. Coogan, and H. S. Gutowsky, J. Chem. Phys. 34, 1191 (1961).

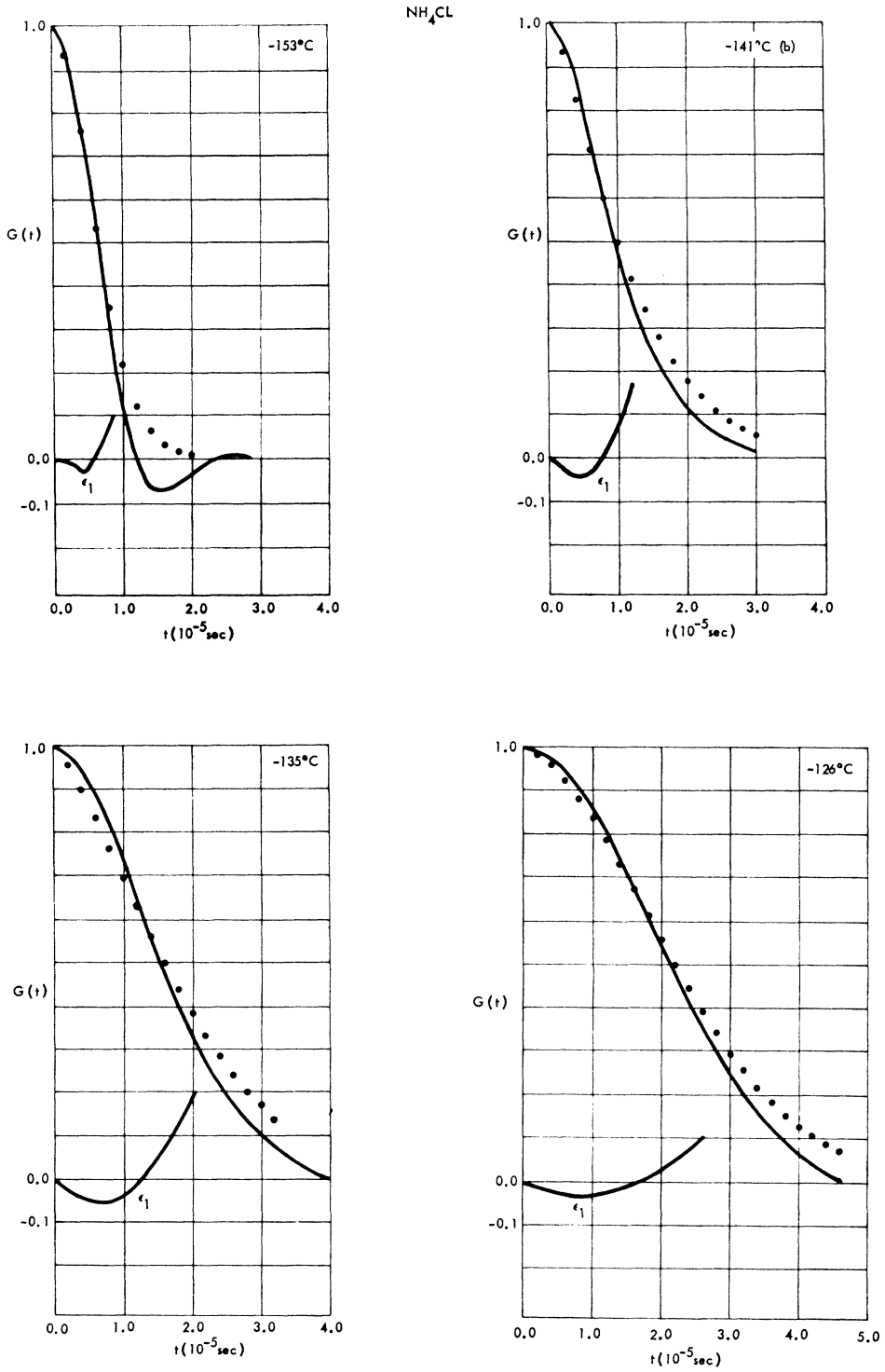

FIG. 2. Comparison of the theoretical relaxation function $G_1(t)$ with the experimental data for NH_4Cl. The full curve is experimental.

A definite high-temperature plateau is not evident below the maximum temperature of 275°C attainable with our apparatus. At that temperature the apparent second moment is about 1/40 of the rigid lattice second moment, and it is apparent that the line is completely narrowed at elevated temperatures. It is appropriate to set $\sigma_B^2=0$.

The relaxation functions for several temperatures are shown in Fig. 4. Beats are exhibited by $G(t)$ at rigid lattice temperatures. These beats occur with a quasi-

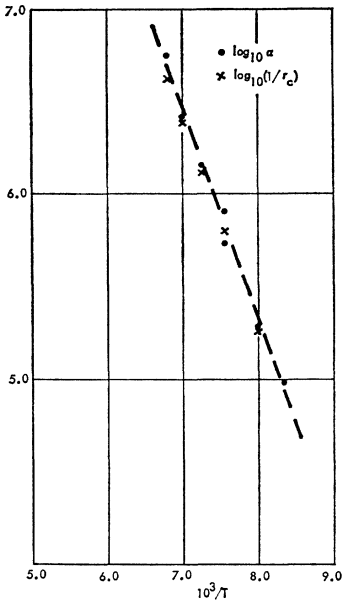

FIG. 3. Arrhenius plot of frequency factors for NH_4Cl. The dashed line is a least-squares fit of the α data. The data resulting from Eq. (26) are designated by x.

angular frequency of 1.9×10^5 sec^{-1}, which is comparable to the root-mean-square linewidth. Since the spectra have no fine structure the oscillations in $G(t)$ must be of the type observed by Lowe and Norberg.[5] As the temperature is increased into the transition region, the beat amplitude is attenuated but the beat frequency appears to remain approximately constant or to change more slowly than the amplitude. These observations may be of importance in the development of future theories of motional narrowing.

TABLE II. Arrhenius parameters for reorientation in NH_4Cl.

Source	Ea (kcal/mole)	$\log_{10}\alpha_\infty$	$\log_{10}(1/\tau_c)_\infty$
Equation (18)	5.2±0.2	14.4±0.4	···
Equation (26)	5.1±0.2	···	14.2±0.3
Reference 21	4.74	···	14.3

The times T_2 and the frequencies α as calculated from Eqs. (20) and (18) are given in Table III. Figure 5 compares the experimental relaxation function with the theoretical model at four temperatures within the transition region. The function $\epsilon_1(t)$ previously defined is also plotted as a quantitative comparison.

Again, for the purpose of comparison with the more usual way of analysis, the graph of $\log_{10}\alpha$ versus $10^3/T$ is shown in Fig. 6 along with the $\log_{10}(1/\tau_c)$ data. The dashed line in Fig. 6 is a least-squares fit of the $\log_{10}\alpha$ data. The results are summarized in Table IV and compared with the results reported in Ref. 22. The values taken from Ref. 22 refer to composition $TiH_{1.933}$, while the present results are for composition $TiH_{1.94}$. The difference in hydrogen content could account for the difference in the activation energy as perhaps could the impurity content of the sample used here.

C. Discussion

The relaxation function $G_1(t)$ was derived in Sec. II from a model which treated the number of fluctuations

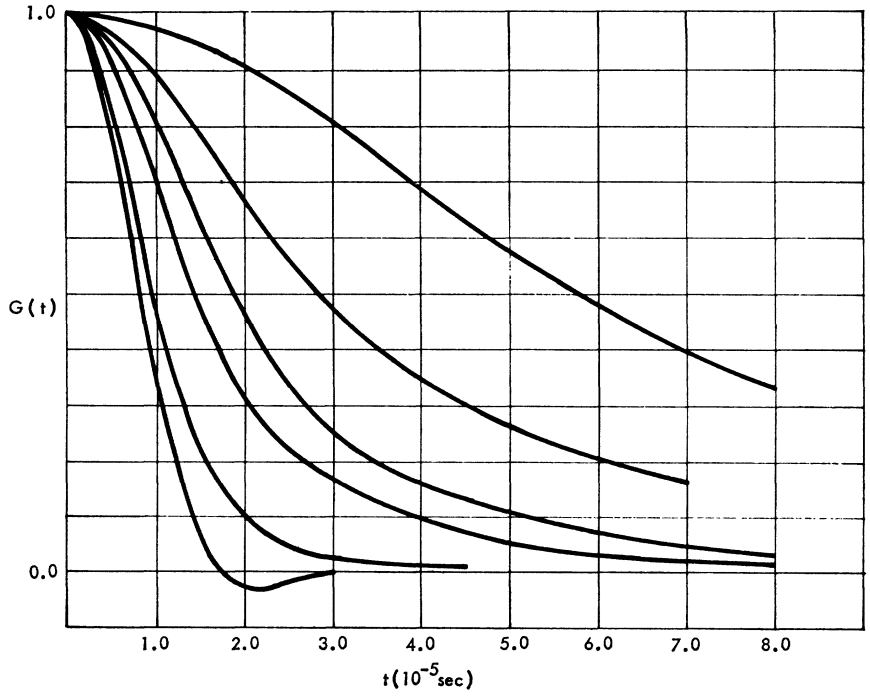

FIG. 4. Experimental relaxation functions $G(t)$ for $TiH_{1.94}$. The sequence of curves from left to right corresponds to the temperature sequence T°C=26, 191.6, 225.7, 241.2, 261.2, and 273.2.

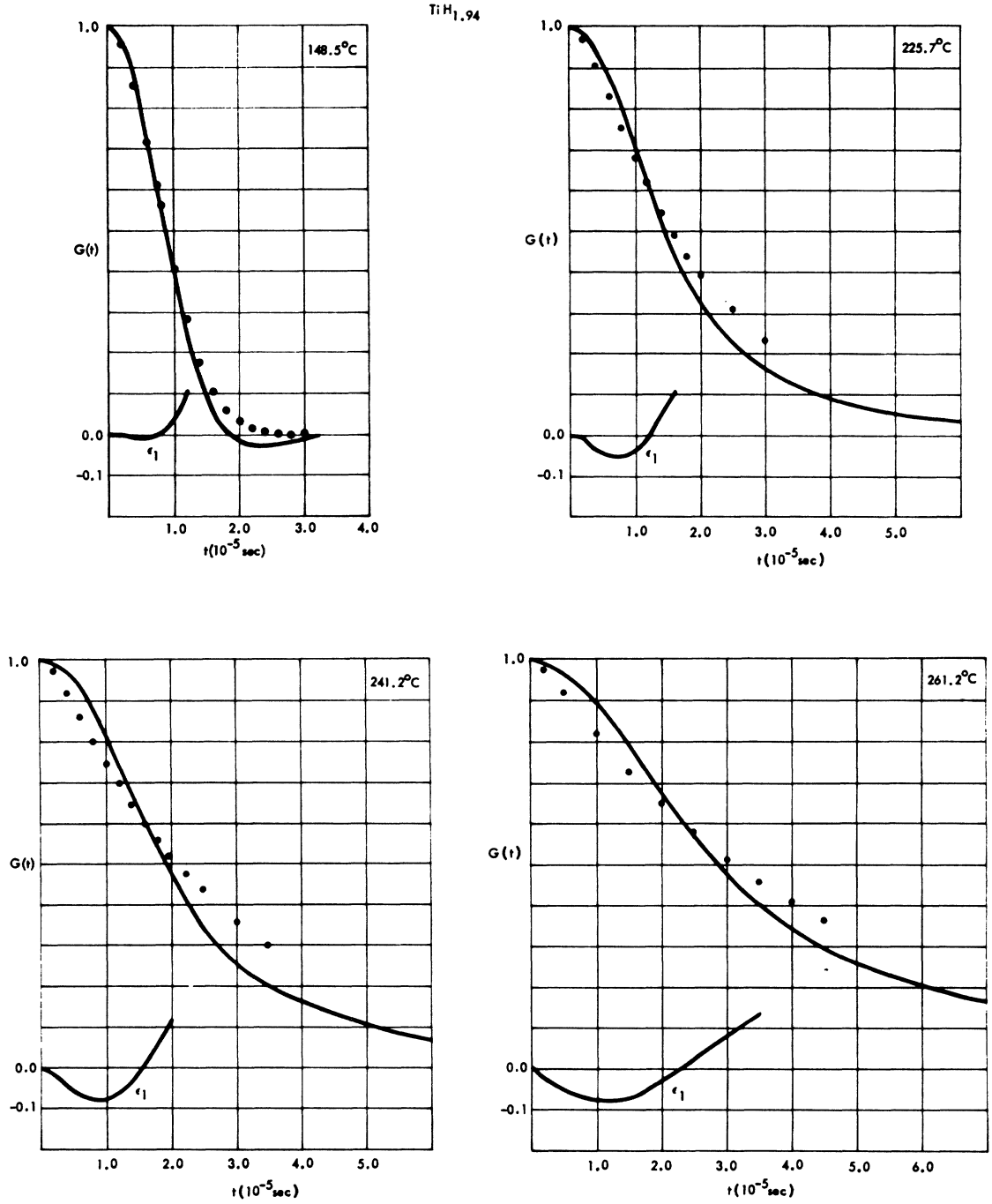

FIG. 5. Comparison of the theoretical relaxation function $G_1(t)$ with the experimental data for $TiH_{1.94}$. The full curve is experimental.

in $\omega(t)$ as being Poisson-distributed. The relaxation function is given by the characteristic function of the integral process $\Phi(t)$ which in this case has an undetermined probability distribution. The function $G_1(t)$ was derived as an approximation which was expected to be valid only up to times approximately equal to T_2. Alternatively, $G_1(t)$ may be derived as the exact relaxation function for a Gaussian process with a covariance given by Eq. (14), and in which the significance of the parameter α is undetermined.[4]

The qualitative validity of the model is revealed by Eq. (18). The quantity $2/T_2$ is descriptive of the width of $g(\omega)$ near half-intensity. As α is increased, $(1/T_2)^2$ decreases from its maximum value $\sigma_A^2+\sigma_B^2$ to the

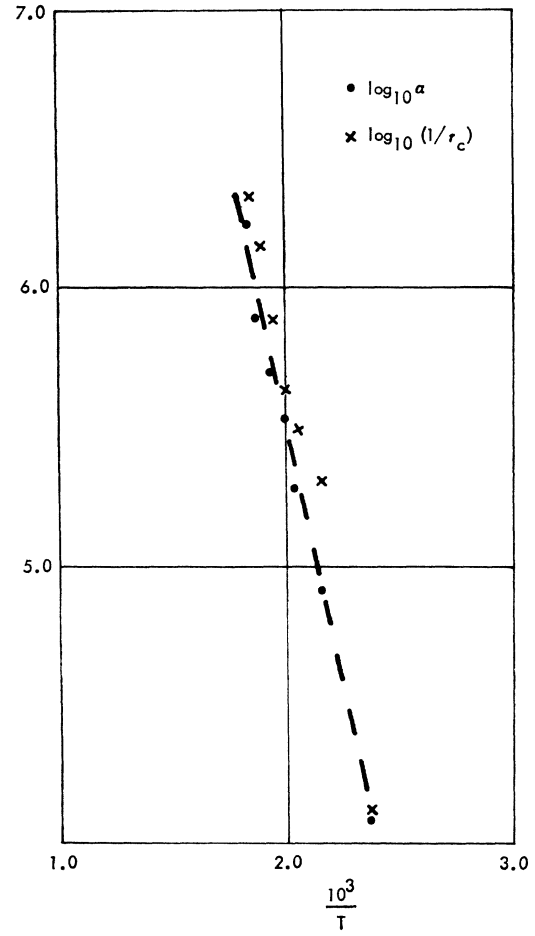

FIG. 6. Arrhenius plot of frequency factors for $TiH_{1.94}$. The dashed line is a least-squares fit of the α data. The data resulting from Eq. (26) are designated by x.

minimum value σ_B^2. One approach to the correlation of the spectral data with the atomic motion is to assume equality between $(1/T_2)^2$ and the observed second moment of the spectrum throughout the transition region. The validity of this assumption will be established shortly. This approach has the advantage that no assumptions regarding the line shape are made.

TABLE III. Values of T_2, α, and M_2 for $TiH_{1.94}$ throughout the transition region. T_2 is the time for which the experimental G is $e^{-1/2}$. α is then calculated from Eq. (18). All values are corrected for modulation effects.

T (°C)	T_2 (10^{-5} sec)	α (10^5 sec)	M_2 (10^{10} sec^{-2})
<100	0.72	···	1.83
148.5	0.75	0.121	1.70
191.6	0.82	0.805	1.53
208.2	0.96	1.90	1.14
225.7	1.22	3.40	0.72
241.2	1.58	5.08	0.43
261.2	2.30	7.91	0.23
273.2	4.77	17.40	0.05

TABLE IV. Arrhenius parameters for diffusion in $TiH_{1.94}$.

Source	Ea (kcal/mole)	$\log_{10}\alpha_\infty$	$\log_{10}(1/\tau_c)_\infty$
Equation (18)	17.5±1.0	13.2±0.5	···
Equation (26)	16.5±1.5	···	13.0 ±.07
Reference 22[a]	10.2	···	10.75

[a] These values are for $TiH_{1.933}$.

Also avoided is an arbitrary assignment of a cutoff value to the static component of the local field as was necessary in the derivation of Eq. (19).[1] With this approach no information regarding the line shape is obtained. This approach was applied to the systems NH_4Cl and $TiH_{1.94}$. The results of that analysis are practically the same as those reported for the method to be discussed next and will not be stated separately.

Another procedure is to obtain T_2 by forcing $G_1(t)$ to coincide with $G(t)$ at $t=T_2$. This convention is guided by the expectation that for periods of time such that $\varphi^2 \leq 1$, the higher-order moments of Φ have not grown large enough to contribute excessively to the characteristic function of Φ. As was mentioned in the experimental part, the frequencies α were calculated using this convention. As can be seen from Figs. 2 and 5, the agreement between $G_1(t)$ and $G(t)$ is within 10% for times up to about $1.4T_2$ for NH_4Cl, and $1.3T_2$ for $TiH_{1.94}$. In the range $0 \leq t \leq T_2$, the maximum deviation $-\epsilon_1$ is 0.06 for NH_4Cl and 0.086 for TiH.

The next point of interest concerns the values of T_2 throughout the transition region. For NH_4Cl the rigid lattice value of T_2, 0.5×10^{-5} sec, is in agreement with the value predicted from Eq. (18) by letting α approach zero. As can be seen from the data of Table I, $1/T_2^2$ closely parallels the observed second moment over the entire transition region. At either extreme the function $G_1(t)$ predicts a Gaussian shape function in contradiction with experimental results. The agreement of $1/T_2^2$ with the observed second moment indicates that T_2 is rather insensitive to the detailed shape of the spectrum. Analogous remarks may be made for the $TiH_{1.94}$ system.

TABLE V. Deviations of $G_1(t)$ and $G_2(t)$ relative to $G(t)$ for NH_4Cl at −135°C.

t	ϵ_1[a]	ϵ_2[b]
0.21	−0.027	−0.024
0.41	−0.051	−0.044
0.61	−0.060	−0.050
0.81	−0.056	−0.045
1.01	−0.037	−0.030
1.21	−0.010	−0.015
1.41	+0.028	+0.028
1.61	+0.078	+0.017
1.81	+0.124	+0.017
2.01	+0.189	−0.009
2.21		−0.065
2.41		−0.17

[a] $T_2=1.28\times10^{-5}$, $\alpha=14.40\times10^5$.
[b] $T_2=1.36\times10^{-5}$, $\alpha=16.65\times10^5$.

TABLE VI. Deviations of $G_1(t)$ and $G_2(t)$ relative to $G(t)$ for $TiH_{1.94}$ at 225.7°C.

t	ϵ_1[a]	ϵ_2[b]
0.21	−0.015	−0.014
0.41	−0.041	−0.037
0.61	−0.057	−0.052
0.81	−0.056	−0.053
1.01	−0.033	−0.040
1.21	−0.002	−0.003
1.41	+0.051	+0.023
1.61	+0.116	+0.06
1.81	+0.187	+0.092
2.01		+0.104
2.41		+0.04
2.81		−0.17

[a] $T_2=1.22\times10^{-5}$, $\alpha=3.40\times10^{5}$.
[b] $T_2=1.30\times10^{-5}$, $\alpha=3.82\times10^{5}$.

Beyond $t=T_2$, $G_1(t)$ consistently overestimates $G(t)$. This behavior for large t indicates that the line-shape intensity changes less rapidly in the vicinity of $\omega=0$ than would be predicted by the expression $G_1(t)$. This, in turn, suggests that the probability distribution of Φ is more nearly uniform than Gaussian near $\Phi=0$. The extreme assumption of uniformly distributed phase deviation leads to the theoretical relaxation function $G_2(t)$. Calculations, based on $G_2(t)$, analogous to those based on $G_1(t)$, were performed for both systems. It would be pointless to reproduce the results in their entirety. Rather, selected samples of the results will be discussed briefly.

In the limit $\alpha=0$, $G_2(t)$ exhibits beats of frequency $[3(\sigma_A^2+\sigma_B^2)]^{1/2}$. For NH_4Cl, $G_2(t)$ has a beat frequency of 3.47×10^5 which compares almost exactly with the observed value 3.5×10^5. Titanium hydride exhibits a beat frequency of 1.9×10^5 sec^{-1} to which should be compared the predicted value 2.34×10^5 sec^{-1}. While the beat frequency is reasonably well predicted by $G_2(t)$, the beat amplitudes are predicted to be much larger than those observed.

For narrowed spectra, $G_2(t)$ can be put into much better agreement with $G(t)$ over a larger time interval than can $G_1(t)$. Tables V and VI compare the two functions $G_1(t)$ and $G_2(t)$ by way of listing $\epsilon_1(t)$ and $\epsilon_2(t)$. The ϵ_i are defined by

$$\epsilon_i(t)=[G_i(t)-G(t)]/G(t).$$

Table V lists data for NH_4Cl at −135°C, and Table VI lists data for $TiH_{1.94}$ at 225.7°C. These results are typical for the two systems. It is remarkable that the function $G_2(t)$, which in the limit $\alpha=0$ is the Fourier transform of a rectangular spectrum, describes narrowed spectra so well.

We conclude by answering a question raised by Abragam.[7] Is the increased labor involved in the use of the relaxation function too high a price to pay for the internal consistency afforded by the method? If all that is desired is an activation energy and jump frequencies describing the motion, the answer is yes. This answer should be qualified by the remark that, in instance of poor signal, large modulation amplitudes might be desirable, thereby causing unknown errors in linewidth measurements. If adequate computing facilities are available, the added labor in calculating Fourier transforms is not at all prohibitive. The method of relaxation functions offers a natural and powerful tool for studying the processes responsible for motional narrowing. In particular, subtleties in the NMR line shape may be detected and correlated with the distribution of phase deviation.

APPENDIX

The practice of magnetic field modulation for the purpose of signal detection results in an artificially broadened line. Andrew[23] has derived Eq. (A1), relating the experimental $2n$th moment M_{2n}' and the actual value M_{2n},

$$M_{2n}'=\sum_{k=0}^{n}\frac{(2n)!b^{2k}}{2^{2k}k!(k+1)!}\frac{M_{2n-2k}}{(2n-2k)!},\qquad\text{(A1)}$$

where b is the modulation amplitude multiplied by the gyromagnetic ratio. The moments are given in units of angular frequency. Equations (23a) and (23b) are special cases of (A1). Halbach[24] has extended Andrew's result to include the effect of modulation frequency. Here the modulation frequency is assumed to be negligibly small.

The Fourier transform $F(t)$ of the artificially broadened line may be expanded in terms of the experimental second moments:

$$F(t)=\sum_{n=0}^{\infty}(-)^n\frac{M_{2n}'}{(2n)!}t^{2n}.\qquad\text{(A2)}$$

The substitution of (A1) in (A2) results in Eq. (A3):

$$F(t)=\sum_{n=0}^{\infty}\sum_{k=0}^{n}(-)^n\frac{(bt)^{2k}}{2^{2k}k!(k+1)!}\frac{M_{2n-2k}}{(2n-2k)!}t^{2n-2k}.\qquad\text{(A3)}$$

The terms in Eq. (A3) may be arranged conveniently in a table in which the rows are labeled by n and the columns by k. As it is written, the series in Eq. (A3) is a sum by rows. The equivalent sum by columns gives

$$F(t)=\sum_{k=0}^{\infty}(-)^k\frac{(bt)^{2k}}{2^{2k}k!(k+1)!}\sum_{n=0}^{\infty}(-)^n\frac{M_{2n}}{(2n)!}t^{2n}.\qquad\text{(A4)}$$

The infinite series indexed by n is the Taylor expansion of $G(t)$. The infinite series indexed by k is $2\times J_1(bt)/(bt)$, where $J_1(bt)$ is the first-order Bessel coefficient. Equation (23c) follows immediately.

It is of some interest to obtain a relation between the shape of the broadened line and the actual line shape.

[23] E. R. Andrew, Phys. Rev. **91**, 425 (1953).
[24] K. Halbach, Phys. Rev. **119**, 1230 (1960).

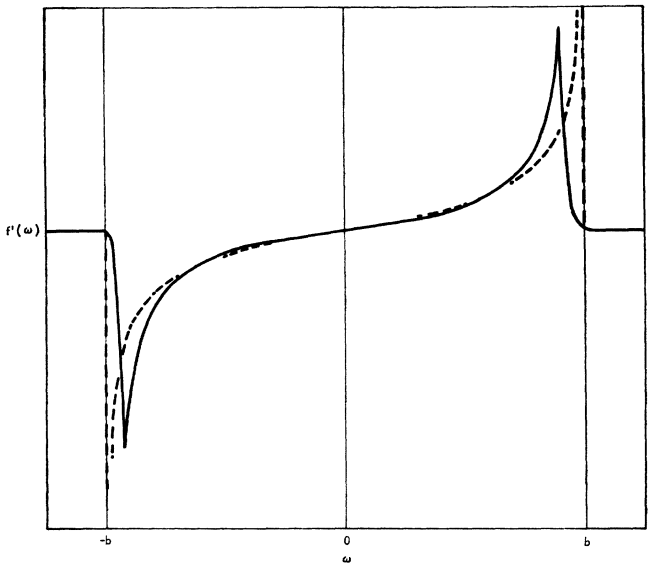

FIG. 7. Recorded signal, solid line, of a narrow water resonance compared with $f'(\omega)$, dashed line, of Eq. (A10). A peak-to-peak modulation amplitude of 2.6 G was used.

The first-order Bessel coefficient may be expressed in integral form as[25]

$$\frac{2J_1(bt)}{bt}=\frac{2}{\pi}\int_{-1}^{1}\cos(btz)[1-z^2]^{1/2}dz. \tag{A5}$$

The function $j(z)$ is defined by

$$\begin{aligned} j(z)&=2[1-z^2]^{1/2}, \quad |z|\leq 1 \\ &=0, \qquad\qquad |z|>0. \end{aligned} \tag{A6}$$

Let $2J_1(bt)/bt$ be denoted by $J(bt)$. Equation (A5) may be rewritten as

$$J(bt)=\frac{2}{\pi}\int_{0}^{\infty}\cos(btz)j(z)dz. \tag{A7}$$

Thus, $J(bt)$ and $j(z)$ are Fourier transform pairs. The relation between the observed line shape $f(\omega)$ and $F(t)$ is Eq. (3) with $G(t)$ replaced by $F(t)$, and $g(\omega)$ by $f(\omega)$.

The desired result is obtained by taking the Fourier cosine transform of Eq. (23c) and applying the convolution theorem for Fourier transforms. Thus,

$$\int_0^\infty J(bt)G(t)\cos\omega t\,dt = \frac{1}{b}\int_0^\infty g(y)\left[j\left(\frac{\omega-y}{b}\right)+j\left(\frac{\omega+y}{b}\right)\right]dy. \tag{A8}$$

Since $g(y)$ and $j(z)$ are even functions, the right-hand side of (A8) simplifies. The transform of Eq. (23c) becomes

$$\int_0^\infty \cos\omega t\,F(t)dt=\int_{-\infty}^{\infty}g(\omega-bx)j(x)dx$$

or

$$f(\omega)=\frac{2}{\pi}\int_{-1}^{1}g(\omega-bx)[1-x^2]^{1/2}dx. \tag{A9}$$

Equations (23c) and (A9) are equivalent. Their validity rests on the validity of Andrew's expansion of the shape function as a Taylor series.[23] Halbach's work[24] shows that such an expansion is valid if the linewidth, frequency of modulation, and amplitude of modulation are small compared to the resonance frequency, and if saturation is absent.

The corrective factor which must be applied to $F(t)$ becomes infinite at the zeros of $J_1(bt)$. The first zero occurs for $bt_0=3.832$. For $t\geq t_0$ the effect of modulation becomes intolerable. If T_2 is to be retrievable from the experimental data, t_0 should be greater than T_2. This is accomplished by using a modulation amplitude such that $bT_2<3.8$.

For the purpose of determining a reasonable lower limit for b, consider the quantity

$$R(t)=[G(t)-F(t)]/G(t)=1-J(bt).$$

For small values of bt, R is approximately equal to $\frac{1}{8}(bt)^2$. Next, let T_2' be defined such that $F(T_2')=G(T_2)$. If T_2-T_2' is small, simple analysis shows that

$$(T_2-T_2')/T_2\approx R(T_2)$$

in the case of a line shape which is actually Gaussian, and that

$$(T_2-T_2')/T_2\approx 2R(T_2)$$

[25] E. T. Whittaker and G. N. Watson, *A Course of Modern Analysis* (Cambridge University Press, New York, 1958), 4th ed., Chap. XVII, p. 366.

in the case of a line shape which is actually Lorentzian. Most line shapes which occur may be approximated, though often crudely so, by Gaussian or Lorentzian shapes. Thus $R(T_2)$ may be used as an estimate of the relative error in T_2 due to modulation. Conversely, a small predetermined relative error in T_2 may be used to arrive at a suitable modulation amplitude.

By way of example, consider a line shape which is actually Gaussian. A predetermined minimum relative error of 0.02 in T_2 leads to

$$2/(5T_2)<b<3.8/T_2,$$

as an experimentally acceptable range for the modulation amplitude.

The "folding function" of Spry[26] is contained explicitly in Eq. (A9). Consider the response of the lock-in amplifier to a δ function. The recorded signal is

$$\begin{aligned} f'(\omega) &= -\omega/[b^2-\omega^2]^{1/2}, & |\omega| \leq b \\ &= 0, & |\omega| > b. \end{aligned} \tag{A10}$$

Within the limitations of the theory, Eq. (A10) is the "folding function." The transition from (A9) back to (23c) represents, in effect, Spry's unfolding procedure.

Figure 7 shows a comparison of (A10) with the recorded signal from a lightly doped sample of water. The width of the water resonance is narrow and for sufficiently large modulation amplitudes will approximate a δ function. The observed response is very well described by Eq. (A10) over the range $|\omega| \leq 0.75b$. The deviation of the response from Eq. (A10) near $|\omega| = b$ may be ascribed to the fact that the water resonance has a finite width. The results may be considered as partial experimental verification of Eq. (A9) and also Eq. (23c).

[26] W. J. Spry, J. Appl. Phys. 28, 660 (1957).

PHYSICAL REVIEW VOLUME 179, NUMBER 2 10 MARCH 1969

Energy Loss and Straggling in Silicon by High-Energy Electrons, Positive Pions, and Protons*

D. W. Aitken, W. L. Lakin, and H. R. Zulliger
Department of Physics and High Energy Physics Laboratory, Stanford University, Stanford, California 94305
(Received 28 February 1968; revised manuscript received 25 November 1968)

The most probable energy loss and energy-loss straggling are investigated in lithium-drifted silicon for electrons, positive pions, and protons with energies 31.5–767.2 MeV. Very good agreement with theory is obtained with protons and pions. The electron spectra demonstrate effects which can be attributed to the absorption by the detector of a portion of the electron bremsstrahlung radiation. No apparent evidence for a predicted decrease in electron ionization through radiative corrections is observed.

INTRODUCTION

THE high resolution which can be obtained with semiconductor radiation detectors suggests that these devices should be very attractive for use in precise investigations of the ionization process. The deep depletion regions which can be produced by the lithium-drifting process permit the realization of an excellent signal-to-noise ratio, even for charged particles near the minimum ionizing region. If such an investigation is undertaken at relatively high energies, where the density of the ionization column produced by the charged particle remains essentially constant over the dimensions of the active detector region, the same data may be used to reveal details of the trapping, recombination, and other "bulk" properties of the semiconductor material.[1]

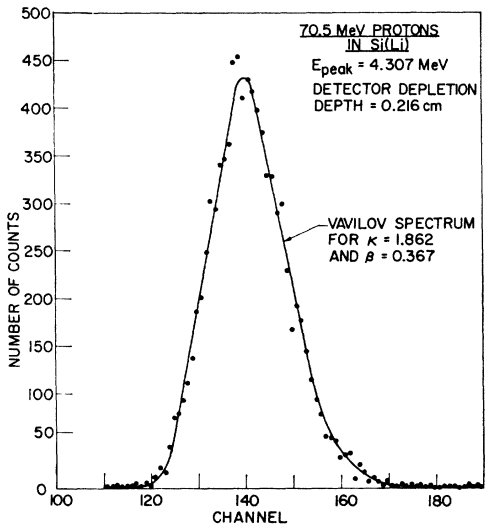

FIG. 1. Experimental and theoretical collision-loss spectra for 70.5-MeV protons in silicon. The parameters κ and β are defined by the kinematics and by the properties of the silicon and the incident particle. The theoretical curve shown is uniquely defined by the experimental parameters, indicating a very good absolute agreement between experiment and theory.

* Work supported in part by the Advanced Research Projctse Agency and monitored by the U. S. Air Force Office of Scientific Research under Contract No. AF 49(638) 1593, and in part by the U. S. Office of Naval Research under Contract No. Nonr-225(67).

[1] D. W. Aitken, D. W. Emerson, and H. R. Zulliger, IEEE Trans. Nucl. Sci. NS-15, 456 (1968).